nature chemical biology

ARTICLE

PUBLISHED ONLINE: 13 JUNE 2010 | DOI: 10.1038/NCHEMBIO.387

Marine antifungal theonellamides target 3β-hydroxysterol to activate Rho1 signaling

Shinichi Nishimura[1,2], Yuko Arita[3,4], Miyuki Honda[3,5], Kunihiko Iwamoto[6], Akihisa Matsuyama[3,7], Atsuko Shirai[3], Hisashi Kawasaki[5], Hideaki Kakeya[1,2], Toshihide Kobayashi[6], Shigeki Matsunaga[8] & Minoru Yoshida[1,3,4,7]*

Linking bioactive compounds to their cellular targets is a central challenge in chemical biology. Here we report the mode of action of theonellamides, bicyclic peptides derived from marine sponges. We generated a chemical-genomic profile of theonellamide F using a collection of fission yeast strains in which each open reading frame (ORF) is expressed under the control of an inducible promoter. Clustering analysis of the Gene Ontology (GO) terms associated with the genes that alter drug sensitivity suggested a mechanistic link between theonellamide and 1,3-β-D-glucan synthesis. Indeed, theonellamide F induced overproduction of 1,3-β-D-glucan in a Rho1-dependent manner. Subcellular localization and *in vitro* binding assays using a fluorescent theonellamide derivative revealed that theonellamides specifically bind to 3β-hydroxysterols, including ergosterol, and cause membrane damage. The biological activity of theonellamides was alleviated in mutants defective in ergosterol biosynthesis. Theonellamides thus represent a new class of sterol-binding molecules that induce membrane damage and activate Rho1-mediated 1,3-β-D-glucan synthesis.

Cyclic and branched cyclic peptides are a large family of natural products with a rich diversity of both structure and activity. They often contain unusual amino acids in the peptide backbone and sometimes possess characteristic modifications in the side chains. Cyclic peptides show a broad range of biological activities including antibacterial, antifungal, immunosuppressive and anticancer activities. Daptomycin, for example, binds bacterial cell membrane and is used as an antibiotic to treat infections caused by Gram-positive bacteria[1]. Antifungal echinocandins including caspofungin and micafungin (FK463) impair cell wall synthesis by inhibiting 1,3-β-D-glucan synthase[2]. Cyclosporin A, which inhibits calcineurin after binding its cellular targets cyclophilins, possesses immunosuppressive activity and is used clinically in organ transplantation[3]. In addition, echinomycin[4,5] and didemnin B[6], which bind DNA and the EF-1α–ribosome complex, exert anticancer activity by inhibiting hypoxia-inducible factor-1 binding to DNA and inhibiting protein synthesis, respectively. Most of these cyclic peptides are synthesized by nonribosomal peptide synthetases, which are widespread among microorganisms. Marine sponges are also an abundant source of this class of bioactive peptides[7].

Theonellamides (TNMs) are members of a unique family of bicyclic dodecapeptides isolated from a marine sponge, *Theonella* sp. These compounds show broad antifungal activity as well as moderate cytotoxicity to mammalian cells[8,9]. Theonegramide[10], theopalauamide and isotheopalauamide[11] are related compounds with minor modifications at specific amino acid side chains. These compounds have a characteristic bicyclic structure bridged by a histidinoalanine residue. A subfamily of compounds contains a sugar group on the imidazole ring at the center of the molecule. The reported biological activities of these compounds were comparable regardless of the presence of the sugar group, suggesting that the characteristic bicyclic peptide framework is responsible for their specific biological actions. Despite screens for binding proteins using TNM-A (**1**) affinity beads[12], their target molecules—that is, those that bind directly to TNMs—remain unknown.

In this study, we screened for genes that confer altered sensitivity to TNM-F (**2**, **Fig. 1a**) in fission yeast cells to gain insight into the mode of action of TNMs. Our screen design took advantage of the fission yeast ORFeome overexpression strain collections[13,14]. Comparison of the chemical-genomic profiles, functional analyses of products of the identified genes and binding assays using a fluorescently labeled theonellamide derivative revealed that TNM-F is a sterol-binding molecule that causes membrane damage and increases cell wall synthesis in a Rho1-dependent manner.

RESULTS

Characterization of TNM-F by chemical-genomic profiling

Screens for binding proteins have already been carried out using TNM-A affinity beads[12]. Thus far, none of the proteins identified appear to be the target responsible for the cytotoxicity. Our group also made TNM affinity beads by a photo-affinity immobilization method[15] and tried to identify the binding proteins from fission yeast cells, but we could not detect any proteins specifically bound to TNM-F (**Supplementary Fig. 1**). We therefore decided to search for chemical-genetic interactions using a set of strains expressing all ~5,000 protein-coding ORFs—the 'ORFeome'—of the fission yeast *Schizosaccharomyces pombe*[13,14], which might provide insights into the genes and pathways targeted by bioactive metabolites. In this collection, each ORF is inserted into the chromosomal *leu1* locus and is expressed as a C-terminally fused protein with two Flag epitopes and one hexahistidine tag under the control of the *nmt1* inducible promoter, which generally leads

[1]Chemical Genomics Research Group, RIKEN Advanced Science Institute, Saitama, Japan. [2]Division of Bioinformatics and Chemical Genomics, Graduate School of Pharmaceutical Sciences, Kyoto University, Kyoto, Japan. [3]Chemical Genetics Laboratory, RIKEN Advanced Science Institute, Saitama, Japan. [4]Graduate School of Science and Engineering, Saitama University, Saitama, Japan. [5]Department of Green and Sustainable Chemistry, Tokyo Denki University, Tokyo, Japan. [6]Lipid Biology Laboratory, RIKEN Advanced Science Institute, Saitama, Japan. [7]CREST Research Project, Japan Science and Technology Corporation, Saitama, Japan. [8]Graduate School of Agricultural and Life Sciences, The University of Tokyo, Tokyo, Japan. *e-mail: yoshidam@riken.jp

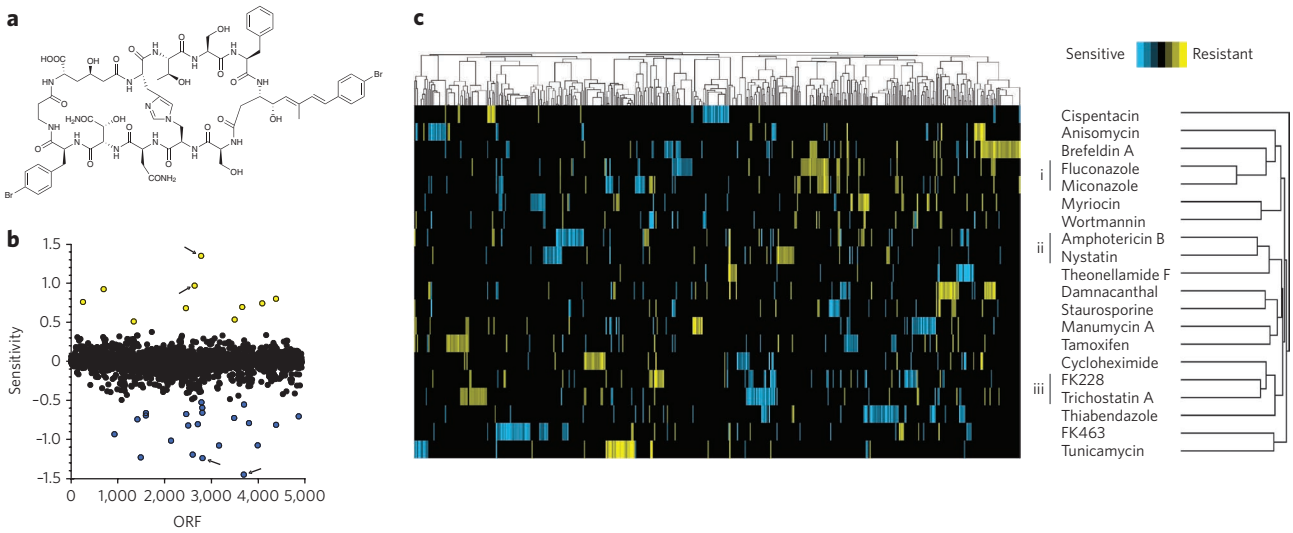

Figure 1 | Generation of chemical-genomic profiles. (**a**) Chemical structure of TNM-F. (**b**) Chemical-genomic profile of TNM-F. Ten ORFs conferring resistance (yellow) and 22 conferring hypersensitivity (blue) were identified (see **Supplementary Table 2** for detail). The *y* axis indicates the $\log_2$ of normalized AUC values, which were obtained from the growth curve of the corresponding transformant in the presence of various concentrations of TNM-F. Arrows indicate representative interactions: *SPCC23B6.04c* and *SPBC23G7.06c* are the top two resistance-conferring ORFs, whereas *SPAC26A3.09* (also known as *rga2*) and *SPAC17G8.14c* (also known as *pck1*) are the top two ORFs conferring hypersensitivity (see **Supplementary Fig. 2**). (**c**) Two-dimensional hierarchical clustering analysis of the 20 compound profiles. Compounds showing similar chemical-genomic profiles were clustered on the vertical axis; 575 ORFs are plotted on the horizontal axis on the basis the degree of hypersensitivity (blue) and resistance (yellow). Compounds possessing same target molecules are labeled with Roman numerals.

to overexpression of the gene product (**Supplementary Fig. 2**). Only a small subset, consisting of 169 strains that showed severe growth retardation upon overexpression, was excluded from our analysis (**Supplementary Data Set 1**). The overexpression strains were exposed individually to TNM-F and a compendium of ten reference compounds with known targets at various concentrations (**Supplementary Fig. 2** and **Supplementary Table 1**). Cell viability in liquid culture was measured using a colorimetric assay (XTT kit) and ranked quantitatively (**Supplementary Data Set 2**). Strains showing a significantly altered sensitivity compared to the control strain were selected and tested two more times. ORFs corresponding to the strains that were positive in all three rounds of screens were subjected to functional analysis (**Fig. 1b**, **Supplementary Data Set 3**).

We analyzed the chemical-genomic profiles by two-dimensional hierarchical clustering analysis[16] and compared the results with those obtained with TNM-F. The dendrogram suggested that these 11 compounds each function via distinct mechanisms (data not shown). To increase the profiles of target-known compounds, we selected approximately 600 strains that showed significant interactions with at least one of the 11 compounds and generated chemical-genetic profiles of nine other compounds using the selected strains (**Supplementary Table 1** and **Supplementary Data Set 4**). Thus, a total of 20 profiles were obtained, which we analyzed by two-dimensional hierarchical clustering analysis (**Fig. 1c**, **Supplementary Fig. 3** and **Supplementary Data Set 5**). We found a weak correlation with polyene antifungals amphotericin B (AMB) and nystatin (correlation coefficient = 0.18), implying that the mode of action of TNM-F is partially shared with these sterol binders.

In addition to pattern-matching analysis, information about the function of genes that alter sensitivity to the query compound (in other words, the hit genes) should be useful in predicting the target or its pathway. In the case of TNM-F, the gene conferring the strongest resistance was *SPCC23B6.04c*, which is predicted to encode a Sec14 homolog (**Supplementary Table 2**). The most sensitive strain overexpressed *SPAC26A3.09*, which encodes a homolog of Rho-type GTPase activating protein Rga2. The second most sensitive overexpressed *pck1*, which encodes a protein kinase C homolog that regulates 1,3-β-D-glucan synthesis[17].

We next determined GO terms with statistically significant enrichment ($P < 0.02$) in the hit genes for the initially tested 11 compounds and ranked them on the basis their extent of enrichment (**Supplementary Data Set 6**). This analysis showed that the hit genes for TNM-F were most enriched for GO terms related to cell polarity and signal transduction. However, none of these hit gene products appeared to be the primary target of TNM, because no physical interaction with immobilized TNM was detected (**Supplementary Fig. 1**). Furthermore, we carried out two-dimensional hierarchical clustering analysis of the enriched GO terms to compare with target-known compounds and found a modest linkage (correlation coefficient = 0.35) between TNM-F and FK463, a frontline clinical antifungal drug that inhibits the synthesis of 1,3-β-D-glucan[18] (**Supplementary Fig. 4**).

Counteraction of TNM-F with FK463

Of 32 TNM-F hit genes, 12 genes were in common with FK463, suggesting that modes of action of TNM-F and FK463 are functionally related (**Fig. 2a**). In contrast, TNM-F shared only two hit genes with nystatin. To see whether TNM-F also affects 1,3-β-D-glucan synthesis, we compared morphology of the cells after drug exposure. FK463 induced cell lysis at the growing ends in fungi by disrupting cell wall integrity (**Fig. 2b**), whereas TNM-F cells did not show any signs of cell lysis (**Fig. 2c**,**d**). Unexpectedly, however, calcofluor white (Cfw) staining showed strong signals at the growing ends and/or the medial region of the cells treated with TNM-F (**Fig. 2c**,**d**). Because TNM-F failed to increase the fluorescence in the *bgs1* mutant[19], in which the activity of the encoded 1,3-β-D-glucan synthase is greatly reduced (**Fig. 2e**,**f**), we suspected that the strong Cfw staining was due to increased 1,3-β-D-glucan synthesis. Similar images were also obtained using another fluorescent dye, aniline blue, which binds specifically to 1,3-β-D-glucans (**Supplementary Fig. 5**)[20]. AMB and nystatin did not increase the Cfw signal (**Fig. 2g**). Notably, the addition of TNM-F following FK463 treatment rescued the cells from FK463-induced cell lysis (**Fig. 2h**). Thus, TNM-F appears to

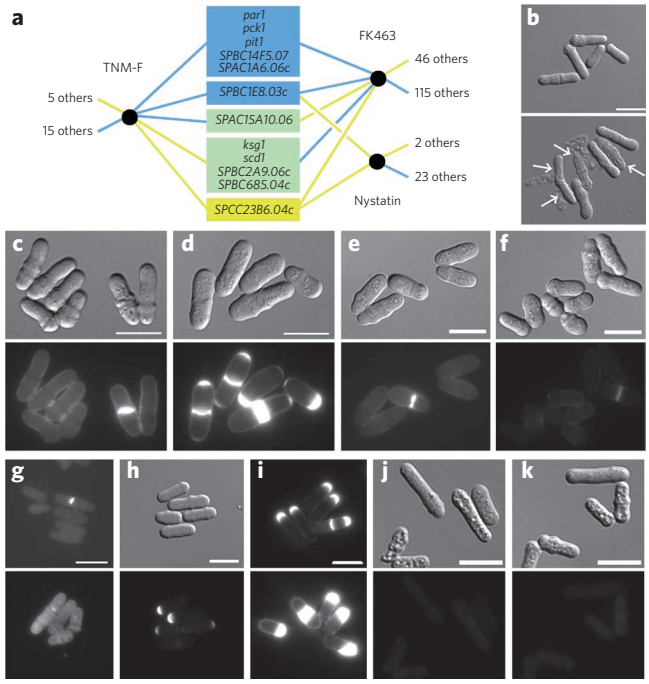

Figure 2 | Cell wall abnormality predicted by GO term analysis. (**a**) Chemical genetic interactions between TNM-F and FK463 or nystatin. Genes whose overexpression conferred resistance are shown in yellow, whereas those whose overexpression conferred hypersensitivity are shown in blue. Green boxes represent genes having opposite effects on TNM-F and FK463. (**b**) Cell lysis caused by FK463. Wild-type cells were treated with (lower) or without (upper) FK463 (20 μg ml^{-1}) for 2.5 h in the presence of 1.2 M sorbitol. FK463-treated cells showed the lysis phenotype (arrows). (**c**,**d**) Abnormal cell wall morphology induced by TNM-F. Yeast cells (HM123) were exposed to DMSO (**c**, 0.5% (v/v), solvent for TNM-F) or TNM-F (**d**, 5 μg ml^{-1}) for 2 h. (**e**,**f**) Bgs1 is required for aberrant Cfw staining by TNM-F. The strong Cfw signals were not observed in *bgs1* temperature-sensitive mutant cells incubated with DMSO (**e**, 0.5% (v/v)) or TNM-F (**f**, 5 μg ml^{-1}) at 27 °C for 2 h. (**g**) Effect of polyene antifungals on cell wall synthesis. Wild-type cells were treated with AMB (0.25 μg ml^{-1}, upper) or nystatin (1.6 μg ml^{-1}, lower) for 3 h. (**h**) Counteraction of FK463-induced cell lysis by TNM-F. (**i**–**k**) Involvement of Rho1 in the TNM-F–induced cell wall abnormality. Cells transformed with empty vector (**i**, upper), pREP41-Rho1 (**i**, lower) or pREP81-Rho1T20N (**j**,**k**) were grown at 30 °C for 15 h in MM liquid medium and then challenged with TNM-F (**i**,**k**) or DMSO (**j**) for an additional 2 h. Scale bars, 10 μm. In **c**–**k**, compound-treated cells were fixed and stained with Cfw. In **c**–**f**, **h**, **j** and **k**, differential interference contrast (DIC; upper) and Cfw (lower) images are shown.

counteract FK463 action by enhancing 1,3-β-D-glucan synthesis. Indeed, five genes identified as the hit genes of TNM-F and FK463 oppositely altered sensitivity to these compounds (**Fig. 2a**).

Rho1 mediates TNM-F–induced morphological abnormalities

1,3-β-D-Glucan is synthesized by transmembrane catalytic subunits in the presence of a regulatory subunit, a prenylated Rho1 (ref. 21). Rho1 is a small GTPase that plays a pivotal role in the signaling pathway involved in the regulation of cell polarity and in 1,3-β-D-glucan synthesis in fission yeast[21–23]. To test whether the TNM-induced 1,3-β-D-glucan synthesis is mediated by the activated Rho1 protein, we expressed a wild-type Rho1 in some cells and a dominant-negative Rho1 (Rho1T20N)[23] in others, using an inducible promoter. The overexpression of wild-type Rho1 greatly enhanced the Cfw staining induced by TNM-F (**Fig. 2i**). On the other hand, overexpression of Rho1T20N clearly inhibited the TNM-induced 1,3-β-D-glucan synthesis (**Fig. 2j**,**k**). Thus, the action of TNM-F appears to require Rho1. Rho1's effects are mediated by its interaction with at least three targets: 1,3-β-D-glucan synthase[21] and the protein kinases Pck1 and Pck2 (ref. 17,24), all of which are involved in 1,3-β-D-glucan synthesis. Deletion of neither *pck1* nor *pck2* abolished the increased Cfw staining induced by TNM-F (**Supplementary Fig. 6**). These results suggest that the major pathway to 1,3-β-D-glucan synthesis upon TNM-F treatment is the direct activation of Bgs1 by Rho1. However, Rho1T20N did not suppress the binding and cytotoxicity of TNM (**Supplementary Figs. 7** and **8**), suggesting that aberrant 1,3-β-D-glucan synthesis is not the primary reason for the TNM's cytotoxicity.

TNMs bind to 3β-hydroxysterols

To determine the subcellular localization of the TNM-binding molecule, we synthesized a fluorescently labeled TNM derivative (**3**, **4**, TNM-BF) by conjugating a 4,4-difluoro-5,7-dimethyl-4-bora-3a, 4a-diaza-*s*-indacene-3-propionic acid moiety (BODIPY-FL) to the β-D-galactose moiety of TNM-A (**Supplementary Fig. 9**). TNM-BF was as active as TNM-F in inhibiting cell growth of wild-type *S. pombe* (**Supplementary Fig. 10**). Fluorescence microscopy clearly showed that TNM-BF is distributed at cell tips and in the septation region of cells undergoing cytokinesis (**Fig. 3a**). According to our Localizome dataset (available here: http://www.riken.jp/SPD/index.html), which assigned each of the 4,429 proteins to one of 17 possible subcellular localizations[13], approximately 80 proteins showed similar localization to TNM-BF (**Supplementary Data Set 7**). GO analysis revealed that transmembrane transporters were significantly enriched among these proteins (**Supplementary Table 3**). Transporters and lipid molecules have a close functional relationship (for example, Pma1 (**Fig. 3b**) is a marker for the lipid raft[25], a characteristic membrane microdomain rich in ergosterol and sphingolipids[26]). The proper localization of Pma1 depends on ergosterol biosynthesis[27]. On the basis of these observations, we theorized that the target of TNM could be a lipid molecule distributed in a polarized manner, rather than a protein. A binding assay using plasma membrane lipid components revealed that TNM-BF selectively recognizes ergosterol but not other lipids tested (**Fig. 3c**). In addition to ergosterol, TNM-BF bound to cholesterol, cholestanol and 5α-cholest-7-en-3β-ol (**Fig. 3d**,**e**). In contrast, a ketone group, an α-hydroxyl group or an esterification of the hydroxyl group at C3 position abolished the binding, indicating that TNM recognizes 3β-hydroxysterols (**Fig. 3e**).

Filipin, a fluorescent compound that forms a specific complex with 3β-hydroxysterols in the cell membrane[28], stained the cell periphery and medial region of cells undergoing cytokinesis[29] in a pattern very similar to that of TNM-BF, suggesting that the target of TNM-F in wild-type *S. pombe* is ergosterol, the major sterol in fungi. Double staining showed a clear overlap of the signals for the two compounds, but the region stained with TNM-BF was slightly more confined (**Fig. 3f**).

In vivo ergosterol distribution is regulated in a cell cycle–dependent manner in fission yeast[29], probably as a result of some function of actin[25,30]. Indeed, we also observed that latrunculin A treatment disrupted the polarity of filipin staining (**Supplementary Fig. 11**). Notably, latrunculin A reduced the fluorescent signal of TNM-BF to an almost undetectable level. Similarly, in a strain possessing an *act1* (also known as *cps8*) temperature-sensitive allele[30,31] both filipin and TNM-BF stained the cell tips and around the septum, as observed in wild-type cells at the permissive temperature, but their polarized localization was lost after temperature shift (**Supplementary Fig. 11**). It should be noted that the decrease in TNM-BF fluorescence was again observed in the *act1* mutant cells at 30 °C. It seems possible that proper organization of the sterol-rich membrane domain is required for TNM binding of the cell membrane. Indeed, overexpression of hit genes *scd1* and *rga2*, both

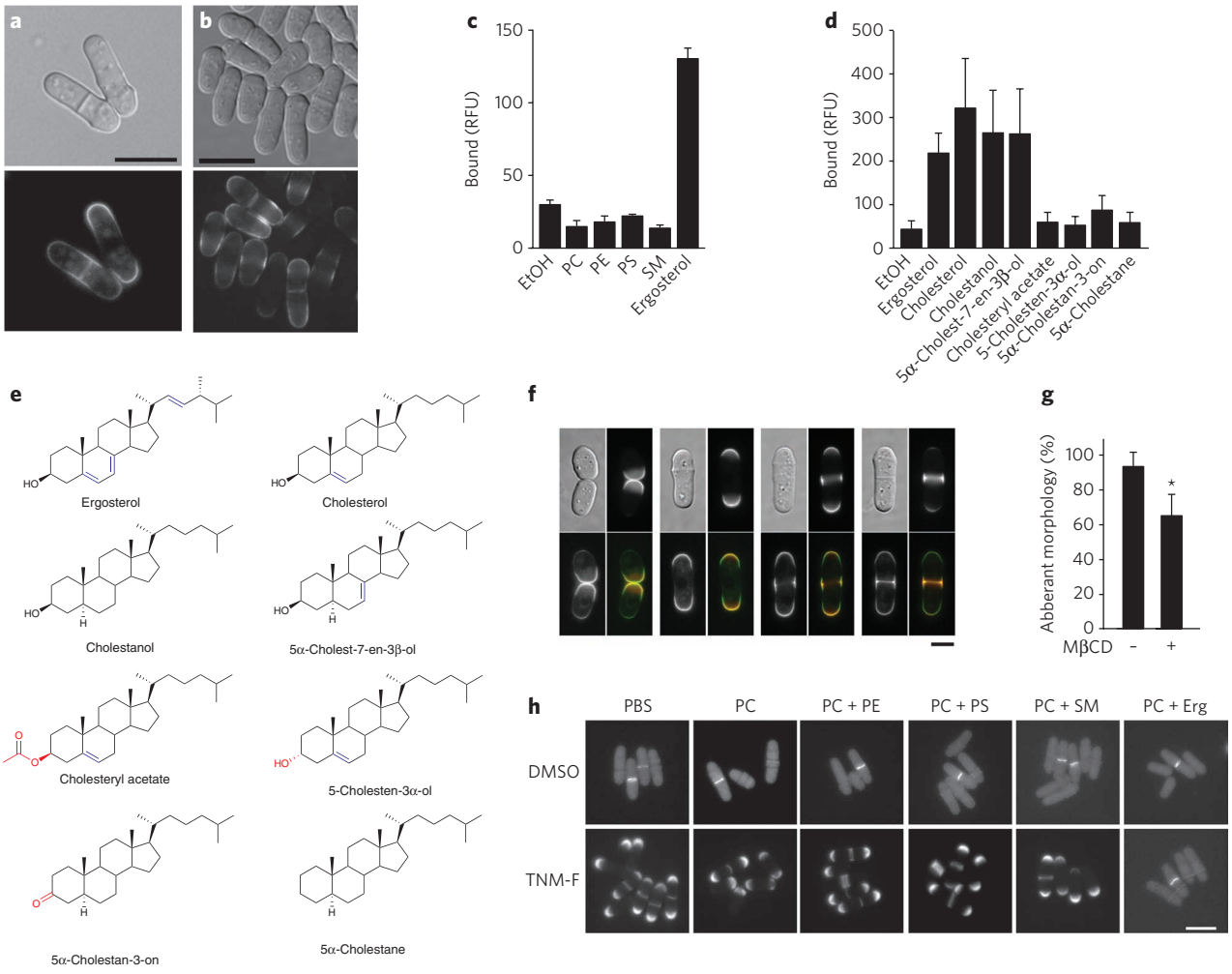

Figure 3 | Identification of 3β-hydroxysterols as the target of TNM-F. (**a**) The fluorescent image of cells stained by TNM-BF. (**b**) An example of protein localization similar to TNM-BF localization. The fluorescent image of the YFP-fused Pma1 is shown. (**c**) Binding of TNM-BF to ergosterol *in vitro*. (**d**) Binding of TNM-BF to various sterols *in vitro*. (**e**) Structure-affinity relationships of sterols. Functionalities colored in blue are not necessary for recognition by TNM-BF, whereas the red-colored structures hamper binding to TNM-BF. (**f**) Co-localization of TNM-BF with filipin. TNM-BF (upper right panels and red in merged images) and filipin (lower left panels and green in merged images) signals were observed in the similar region. Images of cells at different cell cycle stages are shown. (**g**) Effects of ergosterol extraction on the TNM-F–induced cell wall abnormality. Cells were preincubated in the presence (+) or absence (−) of methyl-β-cyclodextrin (MβCD) and then treated with TNM-F. After Cfw staining, cells with abnormally strong signals were counted. Asterisk indicates statistically significant difference ($P < 0.02$). See **Supplementary Figure 13** for details. (**h**) Effects of ergosterol-containing vesicles on TNM-F–induced cell wall abnormalities. Cells were treated with TNM-F (5 μg ml^{-1}) that had been preincubated with POPC vesicles or POPC-based vesicles containing PE (PC + PE), PS (PC + PS), SM (PC + SM) or ergosterol (PC + Erg) for 30 min. After 3 h incubation with TNM-F, cells were fixed and stained with Cfw. Scale bars are 10 μm except that in **f**, which is 5 μm. Data represent means of three (**c**,**d**) or four (**g**, $n > 110$ for each experiment) independent experiments. In **c**,**d** and **g**, error bars indicate s.d. RFU: Relative fluorescence units.

of which are involved in regulation of the actin cytoskeleton[32–34], caused a drastic decrease and increase, respectively, in TNM-BF staining (**Supplementary Fig. 12**).

Sterol binding is required for action of TNM-F

We next determined whether 3β-hydroxysterols are also required for TNM-induced 1,3-β-D-glucan synthesis. First, pretreatment of cells with methyl-β-cyclodextrin, which could extract a substantial amount of ergosterol (**Supplementary Fig. 13**), significantly reduced the number of cells showing an enhanced Cfw signal (**Fig. 3g**). Second, preincubation of TNM-F with 1-palmitoyl-2-oleoyl-*sn*-glycero-3-phosphocholine (POPC)-based multilamellar vesicles did not affect TNM-enhanced Cfw staining, but preincubation with vesicles containing ergosterol abolished it (**Fig. 3h**). These results suggest that pre-absorption of TNM-F with the ergosterol-rich membrane alleviates the action of TNM-F. Furthermore, latrunculin A treatment, which inhibits TNM-BF binding of cells, also hampered the TNM-F–induced abnormal Cfw staining (**Supplementary Fig. 14**). Thus, we conclude that a structured membrane domain rich in ergosterol and related sterols is required for the binding of TNM-F to exert its effects on the cell wall.

Effects of *erg* mutations on TNM-F sensitivity

Genetic mutations in the ergosterol biosynthetic pathway (**Fig. 4a**) have been shown to modulate sensitivity to polyene antibiotics in yeast[27,35]. In *S. pombe erg* mutants, ergosterol production is not detectable; however, filipin staining is not abolished, implying that sterols with filipin-binding activity other than ergosterol can still be produced and that they compensate for the roles of ergosterol[27]. Lack of Erg2, the putative enzyme that converts fecosterol to episterol, or simultaneous deletion of two *erg3*$^+$ homologs, *erg31* and *erg32*, both of which encode putative enzymes catalyzing the

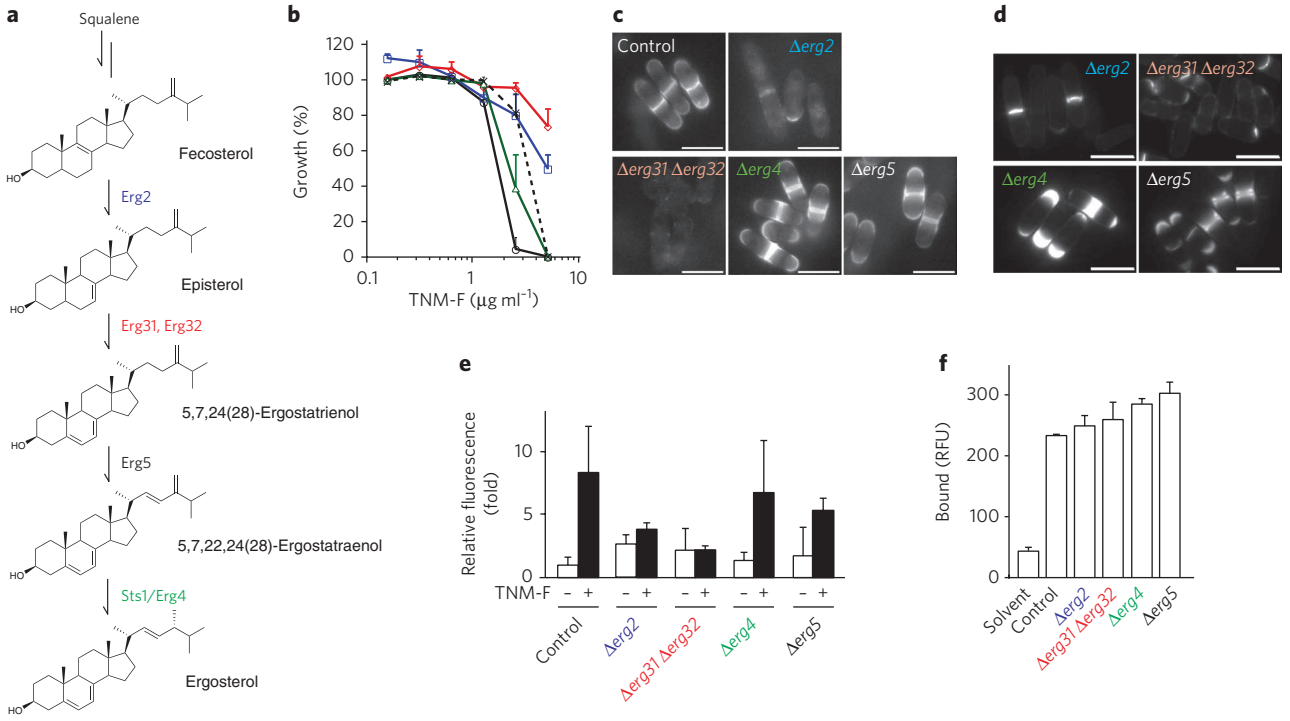

Figure 4 | Genetic interactions with ergosterol biosynthetic genes. (**a**) Ergosterol biosynthesis pathway. (**b**) TNM-F sensitivity of *erg* mutants, Δ*erg2* (solid blue); Δ*erg31* Δ*erg32* (solid red); Δ*sts1/erg4* (solid green); Δ*erg5* (dashed black); and the control strain HM123 (solid black). Data represent means of three independent experiments. Error bars, s.d. (**c**) Localization of TNM-BF-binding molecules in *erg* mutant cells. Cells were treated with TNM-BF (2.5 μg ml^{-1}) at 30 °C for 1 h, and the fluorescence was observed. (**d**,**e**) Effects of mutations in the ergosterol biosynthetic pathway on the TNM-F–induced cell wall abnormality. Various *erg* mutants were treated with TNM-F, and the extent of abnormal cell wall synthesis was determined using Cfw staining. Quantitation of the fluorescence intensity is shown in **e**. Relative intensities to the control cells treated with DMSO were determined. Error bars represent s.d. of three independent experiments ($n \geq 9$ for each experiment). (**f**) Binding of TNM-BF to the sterol fractions prepared from various *erg* mutant cells. Data represent means of three independent experiments. Error bars, s.d.; scale bars, 10 μm.

reaction from episterol to 5,7,24(28)-ergostatrienol, caused ergosterol deficiency and apparent tolerance to polyene antibiotics[27]. These *erg* mutants were also highly tolerant to TNM-F (**Fig. 4b**). On the other hand, deletion of *erg5* conferred modest resistance to TNM-F, and only marginal resistance was observed in Δ*sts1/erg4* cells (**Fig. 4b**). However, deletion of *dsd1* (ref. 36) or *SPBC887.15c*, both encoding enzymes involved in sphingolipid metabolism, did not affect the sensitivity to TNM-F. But Δ*SPBC887.15c* cells were specifically resistant to syringomycin E (**Supplementary Fig. 15**). The ability of TNM-BF to bind to cells correlated well with their sensitivity to TNM-F (**Fig. 4c**). The extent of the abnormality in cell wall architecture in the TNM-F-treated *erg* mutant cells correlated with their TNM sensitivity as well as binding capacity (**Fig. 4d**,**e** and **Supplementary Fig. 16**). However, *in vitro* binding experiments showed similar TNM-BF binding of the sterol fractions isolated from all *erg* deletion strains (**Fig. 4f**), indicating that TNMs bind to other cellular sterols *in vitro*. It is likely that changes in the state of the plasma membrane in the *erg* mutants render TNM-F less readily accessible to membrane sterols. Indeed, the ability to bind to filipin was also reduced in the Δ*erg2* and Δ*erg31* Δ*erg32* cells (**Supplementary Fig. 17**)[27], indicating the modulated accessibility of 3β-hydroxysterols in the membrane of these mutants.

Effects of TNM-F on plasma membrane integrity

To further examine whether TNM binding of the sterol-rich membrane affects yeast plasma membrane integrity, we added the fluorescent dye calcein to the *S. pombe* cells that had been treated with TNM-F for 9 h. Passive entry of calcein over the plasma membrane was observed upon treatment with TNM-F, indicating that cells cannot retain the membrane integrity in the presence of TNM-F (**Fig. 5a**). Calcein diffusion following TNM-F exposure increased in a dose-dependent manner (**Fig. 5b**). Time-course experiments showed that the calcein diffusion into the TNM-F–treated cells gradually increased over time (**Fig. 5c**). In contrast, the elevated 1,3-β-D-glucan synthesis occurred very rapidly, and 1 h treatment was sufficient for the induction of 1,3-β-D-glucan synthesis in most cells at the concentration of 5 μg ml^{-1}(**Supplementary Fig. 18**). Consistent with the TNM susceptibility (**Fig. 4b**), binding (**Fig. 4c**) and Cfw staining (**Fig. 4d**,**e**) data, no significant diffusion of calcein was observed in Δ*erg2* and Δ*erg31* Δ*erg32* cells (**Fig. 5d**), suggesting a direct link between TNM-F binding and the observed effects, including loss of membrane integrity.

Comparison with polyene antifungals

Lastly, we asked whether the mode of action of TNM is identical to that of the conventionally used polyene antibiotics. The most typical morphological change of yeast cells after treatment with polyene antibiotics is the enlargement of vacuoles (**Fig. 5e**,**f**)[37]. This phenomenon was not observed in the TNM-F–treated cells; instead, the vacuoles became highly fragmented (**Fig. 5g**). In contrast to the vacuoles of AMB-treated cells, which leaked vacuolar-specific dye (CDCFDA) to the cytosol, the fragmented vacuoles in the TNM-F-treated cells retained the dye, suggesting that the vacuolar membrane damage is marginal. Rho1 may also be involved in vacuole fragmentation induced by TNM because overexpression of wild-type Rho1 caused similar vacuole fragmentation, and Rho1T20N alleviated the TNM-induced vacuole abnormality (**Supplementary Fig. 19**).

The other characteristic aspect of polyene antifungals is their acute fungicidal effect: most cells died shortly after AMB treatment, and no

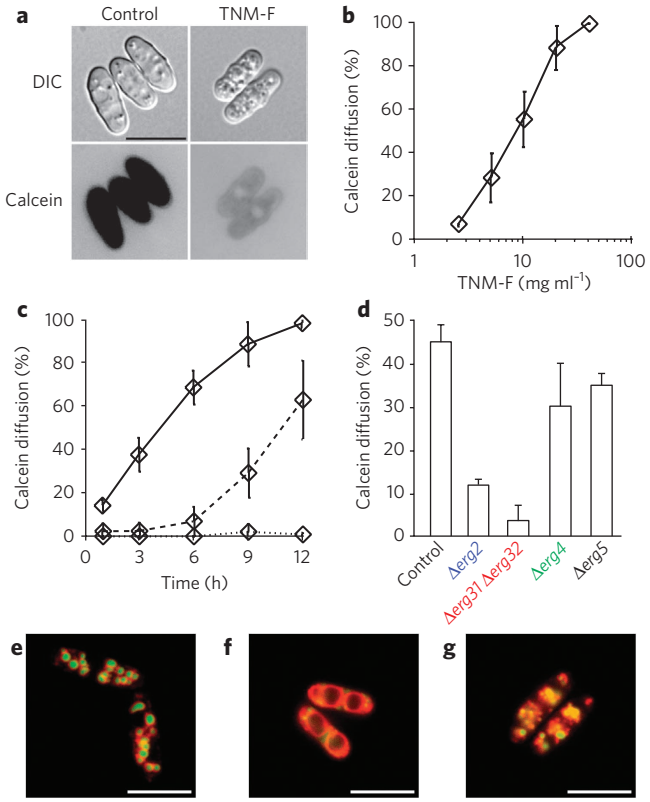

Figure 5 | Disruption of plasma membrane integrity by TNM-F. (**a**) Dye exclusion assay for testing plasma membrane integrity using calcein, a membrane-impermeable fluorescent dye. Passive entry of calcein into *S. pombe* cells was induced by TNM-F (20 μg ml^{-1} for 9 h). In the absence of TNM-F, calcein diffusion was rarely observed. (**b**,**c**) Kinetics of calcein diffusion induced by TNM-F. The dye diffusion was observed in a manner dependent on concentration (**b**) and time (**c**). Incubation time in **b** was 9 h. Cells were incubated without (dotted line) or with 5 μg ml^{-1} (dashed line) or 20 μg ml^{-1} (solid line) of TNM-F in **c**. (**d**) Effects of *erg* mutations on TNM-F–induced membrane damage. Calcein diffusion was attenuated in Δ*erg2* or Δ*erg31* Δ*erg32* cells. Data in **b**–**d** represent means of three independent experiments ($n > 10$ for each experiment). Error bars, s.d. (**e**–**g**) Changes in vacuole morphology. Wild-type cells stained with CDCFDA (green) and FM4-64 (red) were exposed to DMSO (**e**, 1% (v/v)), AMB (**f**, 5 μg ml^{-1}) or TNM-F (**g**, 10 μg ml^{-1}) for 1 h. Scale bars, 10 μm.

time-dependent cell death was observed (**Supplementary Fig. 20**). In contrast, TNM-F showed time-dependent toxicity, with similar kinetics to that of the calcein diffusion (**Fig. 5c** and **Supplementary Fig. 20**). Taken together with the inability of AMB or nystatin to increase 1,3-β-D-glucan synthesis (**Fig. 2g**), these data caused us to conclude that TNM-F is a previously undescribed sterol-binding molecule and that its mode of action is distinct from that of polyene antibiotics.

DISCUSSION

Marine invertebrates, including marine sponges, are an important source for numerous biologically active compounds, which are often synthesized by symbiotic microorganisms[38]. Bicyclic peptides, such as theonellamides (TNMs), are a family of marine natural products with potent antifungal activity. Despite extensive efforts to isolate the TNM-binding proteins, the modes of action of these compounds have been heretofore unknown. Recently, a mutation in *MVD1*, also known as *ERG19*, encoding an essential enzyme involved in an early step in the ergosterol biosynthesis pathway was shown to be specifically resistant to theopalauamide in *Saccharomyces cerevisiae*[39], suggesting a link between the drug target and the ergosterol biosynthetic pathway. In this study, by taking advantage of a chemical-genomic screen for the genes that alter TNM sensitivity when overexpressed, we demonstrated that TNM specifically binds to a class of lipid molecules (3β-hydroxysterols), rather than a protein, in the fission yeast.

The idea that ergosterol, the major sterol molecule in fungi, is the target of TNM in fission yeast is supported not only by the compound's physical interaction with 3β-hydroxysterols, including ergosterol, but also by several lines of genetic and biochemical evidence. Mutants defective in ergosterol biosynthesis (Δ*erg2* and Δ*erg31* Δ*erg32*) showed drastically increased tolerance to TNM and a decreased ability of the cells to bind TNM. Drug sensitivity was well correlated with *in vivo* TNM binding of the membrane. Indeed, TNM-BF binding of the cells overexpressing *SPCC23B6.04c*, the gene conferring the highest resistance, was very low (**Supplementary Fig. 12**). In contrast, *in vitro* binding of TNM-BF to the extracted sterol fraction was independent of susceptibilities of the *erg* mutants, suggesting that TNM-BF binds to sterol metabolites other than ergosterol *in vitro*, and that the accessibility of these 3β-hydroxysterols and the membrane architectures determine the efficient binding of TNM to the plasma membrane *in vivo*. The observation that defects in actin impaired polarized distribution of sterols[30] and greatly reduced *in vivo* TNM binding also supports the notion that proper organization of the membrane domain is prerequisite for *in vivo* TNM binding of the membrane sterols.

TNM binding 3β-hydroxysterols in the membrane initially induced overproduction of the cell wall component 1,3-β-D-glucan. *S. pombe* Rho1 GTPase regulates 1,3-β-D-glucan synthase and is required for the maintenance of cell wall integrity and polarization of the actin cytoskeleton[21,23]. Our mutational analyses demonstrated that TNM triggers the onset of signaling mediated by Rho1 GTPase to directly activate 1,3-β-D-glucan synthase. TNM treatment led to rapid accumulation of 1,3-β-D-glucan at the cell tips and the site of cytokinesis (**Fig. 5c** and **Supplementary Fig. 18**), which are essentially the same regions stained by filipin and TNM-BF, implying that 1,3-β-D-glucan synthase is also localized within or adjacent to the lipid microdomains. Rho1 may also be involved in vacuole fragmentation induced by TNM (**Supplementary Fig. 19**).

A later biological consequence of TNM binding the sterol-rich membrane was the induction of membrane damage. Indeed, the dye exclusion assay showed that the integrity of the plasma membrane in *S. pombe* was damaged by TNM in an incubation time–dependent manner, thereby reducing cell viability. Although TNM induced aberrant 1,3-β-D-glucan synthesis by Rho1 activation, it may be independent of the TNM-induced cytotoxic membrane damage, as the overexpression of Rho1T20N did not suppress the TNM-BF binding the cell membrane (**Supplementary Fig. 7**) and cytotoxicity of TNM-F (**Supplementary Fig. 8**). The polyene antifungals also form pores in the lipid bilayer by interacting with ergosterol, thereby causing leakage of cytosolic constituents such as ions[40]. However, the mode of action of TNM-F is apparently distinct from that of polyene antifungals because the phenotypic changes induced by these two families of antifungals are different. Not all the *erg* mutants prevented TNM binding and damage to membrane. What has been established is the correlation between the TNM's effects on cells and its efficient binding to plasma membrane *in vivo* (**Fig. 4** and **Supplementary Fig. 12**). It is most likely that the binding of TNM-F requires not only sufficient content of ergosterol and other 3β-hydroxysterols but also the proper membrane architecture. In that sense, TNM resembles lysenin, a sphingomyelin-specific toxin isolated from the coelomic fluid of the earthworm *Eisenia foetida*, which has been shown to bind clusters of sphingomyelin in the membrane[41]. Thus, TNM represents a previously unknown class of sterol-binding molecules.

In summary, we have discovered that TNM represents a previously undescribed, mechanistically distinct class of sterol-binding molecules, a powerful tool for exploring the function and localization of sterols in cells. It remains to be determined how TNM binds to sterols in plasma membrane *in situ* and activates Rho1-mediated 1,3-β-D-glucan synthesis, as well as other processes that lead subsequently to membrane damage and cytotoxicity. To develop practical antifungal drugs from such large and complex natural products, it will also be critical to perform structure-function relationship studies to identify the minimal chemical structure essential for TNM's biological activity.

METHODS

Chemical compounds. Thiabendazole and damnacanthal were purchased from Wako Pure Chemical Industries. Other compounds for chemical-genomic profiling were purchased from Sigma. FK463 and cispentacin were gifts from A. Fujie, Astellas Pharma. Trichostatin A and FK228 were from the laboratory collection. TNM-F was isolated from a marine sponge *Theonella* sp. as described previously[8]. The fluorescent derivative of TNM was prepared as described in the **Supplementary Methods.** 1,2-Dimyristoyl-*sn*-glycero-3-phosphocholine (DMPC), 1,2-dimyristoyl-*sn*-glycero-3-phosphoethanolamine (DMPE), and methyl-β-cyclodextrin were purchased from Wako Pure Chemical Industries, Ltd. 1-Palmitoyl-2-oleoyl-*sn*-glycero-3-phosphocholine (POPC), 1,2-dimyristoyl-*sn*-glycero-3-phospho-L-serine (DMPS), chicken egg yolk sphingomyelin (SM), cholesterol, cholestanol, 5α-cholest-7-en-3β-ol, cholesteryl acetate, 5α-cholestan-3-on, 5α-cholestane, calcofluor white, filipin, latrunculin A and syringomycin E were from Sigma. Ergosterol was from Nacalai Tesque, 5-cholesten-3α-ol was from Steraloids Inc., calcein was from Dojindo Laboratories and CDCFDA and FM4-64 were from Molecular Probes Inc.

Yeast strains. *S. pombe* strains used in this study are JY1 (h^-), HM123 (h^- *leu1-32*), *erg* mutants (h^- *ura4-C190T leu1-32 erg2::ura4*$^+$, h^- *ura4-C190T leu1-32 erg31::ura4*-FOA^R *erg32::ura4*$^+$, h^- *ura4-C190T leu1-32 erg4::ura4*$^+$, and h^- *ura4-C190T leu1-32 erg5::ura4*$^+$)[27], and KP165 (h^- *leu1-32 bgs1-i2*)[19]. Fission yeast overexpression strains derived from AM2 (h^{90} *leu1-32*) were generated using the multipurpose plasmid pDUAL-FFH1c[42] as described previously[13].

Preparation of chemical-genomic profiles. Overexpression strains were initially grown on SD solid medium at 30 °C for 2–3 d. To allow expression, each strain was subsequently grown in 200 µL of minimal medium in 96-well plates at 30 °C for 48 h with vigorous shaking. Expression-induced cell cultures were diluted at 1:2,000 and exposed to compounds at 30 °C for 24 h in 100 µL minimal medium in 96-well plates. Cell growth was assessed by the degree of respiration (an XTT assay) using a Cell Proliferation Kit II (Roche, Switzerland). Secondary screens were carried out on strains showing significantly altered sensitivity in the primary screen. The sensitivity of the strain was quantified by calculating the area under the curve (AUC) of growth versus dose (*x* axis: compound concentration; *y* axis: cell growth (%)), normalized against the median AUC value of all strains in each experiment. Strains with significantly altered normalized AUC values in the secondary screen were tested again; in this trial, the obtained AUC value was normalized against the AUC value from the control strain (**Supplementary Data Sets 2** and **3**).

Preparation of compound profiles using a minimal strain set. See **Supplementary Methods** for experimental procedures.

Clustering analysis. See **Supplementary Methods** and **Supplementary Dataset 8** for experimental procedures.

Functional analysis of the chemical-genomic profiles with GO terms. See **Supplementary Methods** for experimental procedures.

Lipid binding assay. The ability of TNM-BF to bind to various lipid species was evaluated in a microtiter plate. The wells of microtiter plates (Immulon 1B, Thermo Fisher Scientific, Inc.) were coated with lipid solution (50 µM of DMPC, DMPE, DMPS, sterols (10 µM each), SM (10 µg ml^{-1}), or 40 µl of yeast sterol fractions (10 µg ml^{-1})) in ethanol by evaporating at 30 °C for 2 h. After blocking the wells with Tris-buffered saline (10 mM Tris-HCl, pH 7.4, 150 mM NaCl) containing 1% (v/v) skim milk (BD) (buffer A) for 1 h at 30 °C, the wells were incubated with TNM-BF (1.0 µg ml^{-1}) in buffer A for 1 h at 30 °C. After washing the wells twice with buffer A, we dissolved the bound TNM-BF in 50 µl of DMSO, 40 µl of which was transferred to another 96-well plate (FIA black module plate, Greiner Bio-One) to measure the bound fluorescence (excitation 490 nm, emission 528 nm) using a SpectraMax M2e microplate reader (Molecular Devices). Yeast sterol fractions were prepared as described previously[27].

Drug sensitivity test. See **Supplementary Methods** for experimental procedures.

Microscopy. Cells were treated with compounds at 30 °C unless stated otherwise in the figure legend. Multilamellar vesicle competition was carried out using POPC-based vesicles. In detail, TNM-F (10 µg ml^{-1}) was preincubated with POPC vesicles or POPC-based vesicles (100 µM of total lipid concentration) containing 20 mol % of DMPE, DMPS, SM or ergosterol for 30 min. Cells were incubated with this mixture for 3 h (final concentration of TNM-F is 5 µg ml^{-1} and that of total lipid is 50 µM), then fixed and stained with Cfw. For Cfw staining, fixed cells were suspended in a buffer (100 mM PIPES, pH 6.9, 1 mM EGTA, 1 mM $MgSO_4$) containing Cfw. Cell lysis by FK463 was observed as described in **Supplementary Methods**. Visualization of sterols using filipin was carried out as described[29]. For the co-localization study, cells were exposed to TNM-BF (2.5 µg ml^{-1}) for 30 min, followed by filipin staining. Vacuole morphology was visualized with FM4-64 and CDCFDA as described[43]. Dye exclusion assay was carried in the presence of calcein at a concentration of 50 µg ml^{-1}. To collect images, we used either a DeltaVision system (Applied Precision) with an Olympus IX70 fluorescence microscope equipped with an UPlan Apo ×100 lens, or a MetaMorph system (Universal Imaging Corp.) with an Olympus IX81 fluorescence microscope equipped with an UPLSAPO ×100 lens. Quantitation of the intensity of the Cfw fluorescence was carried out using MetaMorph software.

Received 6 February 2009; accepted 23 March 2010; published online 13 June 2010

References

1. Baltz, R.H. Daptomycin: mechanisms of action and resistance, and biosynthetic engineering. *Curr. Opin. Chem. Biol.* **13**, 144–151 (2009).
2. Denning, D.W. Echinocandin antifungal drugs. *Lancet* **362**, 1142–1151 (2003).
3. Rovira, P., Mascarell, L. & Truffa-Bachi, P. The impact of immunosuppressive drugs on the analysis of T-cell activation. *Curr. Med. Chem.* **7**, 673–692 (2000).
4. Dawson, S., Malkinson, J.P., Paumier, D. & Searcey, M. Bisintercalator natural products with potential therapeutic applications: isolation, structure determination, synthetic and biological studies. *Nat. Prod. Rep.* **24**, 109–126 (2007).
5. Kong, D. *et al.* Echinomycin, a small-molecule inhibitor of hypoxia-inducible factor-1 DNA-binding activity. *Cancer Res.* **65**, 9047–9055 (2005).
6. Vera, M.D. & Joullie, M.M. Natural products as probes of cell biology: 20 years of didemnin research. *Med. Res. Rev.* **22**, 102–145 (2002).
7. Matsunaga, S. & Fusetani, N. Nonribosomal peptides from marine sponges. *Curr. Org. Chem.* **7**, 945–966 (2003).
8. Matsunaga, S., Fusetani, N., Hashimoto, K. & Walchli, M. Theonellamide-F - a novel antifungal bicyclic peptide from a marine sponge *Theonella* sp. *J. Am. Chem. Soc.* **111**, 2582–2588 (1989).
9. Matsunaga, S. & Fusetani, N. Theonellamides A–E, cytotoxic bicyclic peptides, from a marine sponge *Theonella* sp. *J. Org. Chem.* **60**, 1177–1181 (1995).
10. Bewley, C.A. & Faulkner, D.J. Theonegramide, an antifungal glycopeptide from the Philippine lithistid sponge *Theonella swinhoei*. *J. Org. Chem.* **59**, 4849–4852 (1994).
11. Schmidt, E.W., Bewley, C.A. & Faulkner, D.J. Theopalauamide, a bicyclic glycopeptide from filamentous bacterial symbionts of the lithistid sponge *Theonella swinhoei* from Palau and Mozambique. *J. Org. Chem.* **63**, 1254–1258 (1998).
12. Wada, S., Matsunaga, S., Fusetani, N. & Watabe, S. Interaction of cytotoxic bicyclic peptides, theonellamides A and F, with glutamate dehydrogenase and 17beta-hydroxysteroid dehydrogenase IV. *Mar. Biotechnol. (NY)* **2**, 285–292 (2000).
13. Matsuyama, A. *et al.* ORFeome cloning and global analysis of protein localization in the fission yeast *Schizosaccharomyces pombe*. *Nat. Biotechnol.* **24**, 841–847 (2006).
14. Shirai, A. *et al.* Global analysis of gel mobility of proteins and its use in target identification. *J. Biol. Chem.* **283**, 10745–10752 (2008).
15. Kanoh, N., Honda, K., Simizu, S., Muroi, M. & Osada, H. Photo-cross-linked small-molecule affinity matrix for facilitating forward and reverse chemical genetics. *Angew. Chem. Int. Edn Engl.* **44**, 3559–3562 (2005).
16. Hughes, T.R. *et al.* Functional discovery via a compendium of expression profiles. *Cell* **102**, 109–126 (2000).
17. Arellano, M. *et al. Schizosaccharomyces pombe* protein kinase C homologues, pck1p and pck2p, are targets of rho1p and rho2p and differentially regulate cell integrity. *J. Cell Sci.* **112**, 3569–3578 (1999).
18. Tomishima, M. *et al.* FK463, a novel water-soluble echinocandin lipopeptide: synthesis and antifungal activity. *J. Antibiot. (Tokyo)* **52**, 674–676 (1999).
19. Deng, L. *et al.* Phosphatidylinositol-4-phosphate 5-kinase regulates fission yeast cell integrity through a phospholipase C-mediated protein kinase C-independent pathway. *J. Biol. Chem.* **280**, 27561–27568 (2005).
20. Kippert, F. & Lloyd, D. The aniline blue fluorochrome specifically stains the septum of both live and fixed *Schizosaccharomyces pombe* cells. *FEMS Microbiol. Lett.* **132**, 215–219 (1995).
21. Arellano, M., Duran, A. & Perez, P. Rho 1 GTPase activates the (1–3) beta-D-glucan synthase and is involved in *Schizosaccharomyces pombe* morphogenesis. *EMBO J.* **15**, 4584–4591 (1996).

22. Arellano, M., Duran, A. & Perez, P. Localisation of the *Schizosaccharomyces pombe* rho1p GTPase and its involvement in the organisation of the actin cytoskeleton. *J. Cell Sci.* **110**, 2547–2555 (1997).
23. Nakano, K., Arai, R. & Mabuchi, I. The small GTP-binding protein Rho1 is a multifunctional protein that regulates actin localization, cell polarity, and septum formation in the fission yeast *Schizosaccharomyces pombe*. *Genes Cells* **2**, 679–694 (1997).
24. Sayers, L.G. *et al.* Rho-dependence of *Schizosaccharomyces pombe* Pck2. *Genes Cells* **5**, 17–27 (2000).
25. Takeda, T., Kawate, T. & Chang, F. Organization of a sterol-rich membrane domain by cdc15p during cytokinesis in fission yeast. *Nat. Cell Biol.* **6**, 1142–1144 (2004).
26. Simons, K. & Ikonen, E. Functional rafts in cell membranes. *Nature* **387**, 569–572 (1997).
27. Iwaki, T. *et al.* Multiple functions of ergosterol in the fission yeast *Schizosaccharomyces pombe*. *Microbiology* **154**, 830–841 (2008).
28. Drabikowski, W., Lagwińska, E. & Sarzala, M.G. Filipin as a fluorescent probe for location of cholesterol in membranes of fragmented sarcoplasmic reticulum. *Biochim. Biophys. Acta* **291**, 61–70 (1973).
29. Wachtler, V., Rajagopalan, S. & Balasubramanian, M.K. Sterol-rich plasma membrane domains in the fission yeast *Schizosaccharomyces pombe*. *J. Cell Sci.* **116**, 867–874 (2003).
30. Codlin, S., Haines, R.L. & Mole, S.E. btn1 affects endocytosis, polarization of sterol-rich membrane domains and polarized growth in *Schizosaccharomyces pombe*. *Traffic* **9**, 936–950 (2008).
31. Ishiguro, J. & Kobayashi, W. An actin point-mutation neighboring the 'hydrophobic plug' causes defects in the maintenance of cell polarity and septum organization in the fission yeast *Schizosaccharomyces pombe*. *FEBS Lett.* **392**, 237–241 (1996).
32. Villar-Tajadura, M.A. *et al.* Rga2 is a Rho2 GAP that regulates morphogenesis and cell integrity in *S. pombe*. *Mol. Microbiol.* **70**, 867–881 (2008).
33. Chang, E.C. *et al.* Cooperative interaction of *S. pombe* proteins required for mating and morphogenesis. *Cell* **79**, 131–141 (1994).
34. Iwaki, N., Karatsu, K. & Miyamoto, M. Role of guanine nucleotide exchange factors for Rho family GTPases in the regulation of cell morphology and actin cytoskeleton in fission yeast. *Biochem. Biophys. Res. Commun.* **312**, 414–420 (2003).
35. Hampsey, M. A review of phenotypes in *Saccharomyces cerevisiae*. *Yeast* **13**, 1099–1133 (1997).
36. Garton, S., Michaelson, L.V., Beaudoin, F., Beale, M.H. & Napier, J.A. The dihydroceramide desaturase is not essential for cell viability in *Schizosaccharomyces pombe*. *FEBS Lett.* **538**, 192–196 (2003).
37. Takeo, K. *et al.* Rapid, extensive and reversible vacuolation of *Schizosaccharomyces pombe* induced by amphotericin B. *FEMS Microbiol. Lett.* **108**, 265–269 (1993).
38. Piel, J. Bacterial symbionts: prospects for the sustainable production of invertebrate-derived pharmaceuticals. *Curr. Med. Chem.* **13**, 39–50 (2006).
39. Ho, C.H. *et al.* A molecular barcoded yeast ORF library enables mode-of-action analysis of bioactive compounds. *Nat. Biotechnol.* **27**, 369–377 (2009).
40. Bolard, J. How do the polyene macrolide antibiotics affect the cellular membrane properties? *Biochim. Biophys. Acta* **864**, 257–304 (1986).
41. Shogomori, H. & Kobayashi, T. Lysenin: a sphingomyelin specific pore-forming toxin. *Biochim. Biophys. Acta* **1780**, 612–618 (2008).
42. Matsuyama, A. *et al.* pDUAL, a multipurpose, multicopy vector capable of chromosomal integration in fission yeast. *Yeast* **21**, 1289–1305 (2004).
43. Gachet, Y. & Hyams, J.S. Endocytosis in fission yeast is spatially associated with the actin cytoskeleton during polarised cell growth and cytokinesis. *J. Cell Sci.* **118**, 4231–4242 (2005).

Acknowledgments

We thank C. Boone (Univ. Toronto) for sharing unpublished results and discussions, A. Fujie (Astellas Pharma) for kind gifts of FK463 and cispentacin, K. Takegawa (Kyushu Univ.) for *erg* deletion strains, T. Kuno (Kobe Univ.) for the *bgs1* mutant and *pck* deletion strains and K. Nakano (University of Tsukuba) for *rho1*-expression plasmids. We also thank J. Ishiguro (Konan Univ.) for the *act1/cps8* mutant strain, which was provided through the Yeast Genetic Resource Center (YGRC), N. Kanoh, S. Shimizu and H. Osada (RIKEN Advanced Science Institute) for helping in the preparation of TNM affinity beads, J. Ochi (Kyoto Univ.) for technical assistance and J. Piotrowski (RIKEN Advanced Science Institute) for critical reading of the manuscript. We are grateful to the RIKEN Brain Science Institute's Research Resource Center for mass spectrometry. This work was supported in part by the New Energy and Industrial Technology Development Organization Project on Development of Basic Technology to Control Biological Systems Using Chemical Compounds, a Grant-in-Aid from the Ministry of Education, Culture, Sports, Science and Technology of Japan and the Chemical Genomics Research Project, RIKEN Advanced Science Institute.

Author contributions

M.Y. is responsible for project planning and experimental design, with support from K.I., H. Kawasaki, H. Kakeya and T.K.; S.N. performed most of the experiments; Y.A. assisted *in vitro* sterol binding experiments; M.H. assisted chemical-genomic screen; A.M. and A.S. prepared the yeast strain collection; S.M. prepared theonellamides.

Competing financial interests

The authors declare no competing financial interests.

Additional information

Supplementary information, chemical compound information and chemical probe information is available online at http://www.nature.com/naturechemicalbiology/. Reprints and permissions information is available online at http://npg.nature.com/reprintsandpermissions/. Correspondence and requests for materials should be addressed to M.Y.